

Dosimetric properties of improved GafChromic films for seven different digitizers

Slobodan Devic,^{a)} Jan Seuntjens, Gyorgy Hegyi, and Ervin B. Podgorsak
Medical Physics Department, McGill University Health Centre, Montréal, Québec, Canada

Christopher G. Soares
Division of Ionizing Radiation, National Institute of Standards and Technology, Gaithersburg, Maryland 20899

Assen S. Kirov
Memorial Sloan-Kettering Cancer Center, New York, New York 10021

Imad Ali and Jeffrey F. Williamson
Department of Radiation Oncology, Virginia Commonwealth University, Richmond, Virginia 23298

Angel Elizondo
eRadlink Inc., Torrance, California 90505

(Received 26 February 2004; revised 6 June 2004; accepted for publication 7 June 2004; published 13 August 2004)

Two recently introduced GafChromic film models, HS and XR-T, have been developed as more sensitive and uniform alternatives to GafChromic MD-55-2 film. The HS model has been specifically designed for measurement of absorbed dose in high-energy photon beams (above 1 MeV), while the XR-T model has been introduced for dose measurements of low energy (0.1 MeV) photons. The goal of this study is to compare the sensitometric curves and estimated dosimetric uncertainties associated with seven different GafChromic film dosimetry systems for the two new film models. The densitometers tested are: LKB Pharmacia Ultrascan XL, Molecular Dynamics Personal Densitometer, Nuclear Associates Radiochromic Densitometer Model 37-443, Photoelectron Corporation CMR-604, Laser Pro 16, Vidar VXR-16, and AGFA Arcus II document scanner. Pieces of film were exposed to different doses in a dose range from 0.5 to 50 Gy using 6 MV photon beam. Functional forms for dose vs net optical density have been determined for each of the GafChromic film-dosimetry systems used in this comparison. Two sources of uncertainties in dose measurements, governed by the experimental measurement and calibration curve fit procedure, have been compared for the densitometers used. Among the densitometers tested, it is found that for the HS film type the uncertainty caused by the experimental measurement varies from 1% to 3% while the calibration fit uncertainty ranges from 2% to 4% for doses above 5 Gy. Corresponding uncertainties for XR-T film model are somewhat higher and range from 1% to 5% for experimental and from 2% to 7% for the fit uncertainty estimates. Notwithstanding the significant variations in sensitivity, the studied densitometers exhibit very similar precision for GafChromic film based dose measurements above 5 Gy. © 2004 American Association of Physicists in Medicine.
[DOI: 10.1118/1.1776691]

Key words: GafChromic film dosimetry, uncertainty analysis, sensitivity curves

I. INTRODUCTION

The introduction of radiochromic films (based on polydiacetylene) has solved some of the problems associated with conventional 2D radiation detectors. The high spatial resolution, weak energy dependence and near tissue-equivalence of radiochromic films (RCF) make them suitable for measurement of dose distributions in radiation fields with high dose gradients. Initially, GafChromic detectors were developed for dose monitoring in industrial radiation processing.¹⁻⁴ Having only a 6 μm thick sensitive layer, these relatively insensitive films were suitable for relatively high dose measurements in excess of 50 Gy to 2500 Gy and were used for several years for clinical dosimetry research⁵⁻⁸ under the name HD-810 (or DM-1260, Nuclear Associates, Model No. 37-040). A more sensitive GafChromic film, the MD-55 model (Nuclear

Associates, Model No. 37-041), was developed^{9,10} that had a 15 μm thick sensitive layer and covered a dose range from 10 Gy to 100 Gy. Subsequently, an even more sensitive model, the MD-55-2, was introduced that was produced by adding two MD-55 layers together.¹¹⁻¹⁴ The MD-55-2 model covers a dose range from 1 Gy to 250 Gy and is much better adapted to clinical applications¹⁵⁻¹⁹ than its predecessors.

The sensitivity of the MD-55-2 model GafChromic film is relatively high, however, its dose response was reported to be nonuniform by 8%–15%,^{11,12,14} limiting its use in clinical applications. Recently, two new GafChromic film models, the XR-T and HS, have been introduced. The XR-T model has a sensitive layer containing high atomic number Z materials, intended to compensate for the lower absorption cross section of its organic active layer when irradiated with low-

energy photons (below 0.1 MeV). On the other hand, the HS model was designed for high-energy photon beams (above 1 MeV).

A critical component in the GafChromic dose-measurement process is the densitometer used for the film's optical density (OD) readout. Several types of instruments are used for two-dimensional film densitometry. One type consists of a single collimated or focused light beam-detector pair and requires translation of the film and/or light source from point-to-point over the film. The spatial resolution is governed by the light beam diameter and/or detector aperture as well as by the accuracy and spatial sampling rate of the translation mechanism. The second approach uses a one- or two-dimensional position-sensitive light detector to eliminate one or both scanning motions. Some densitometers record a single line of OD measurements at a time using a linear CCD array and translate the film perpendicularly to the scanning axis while other systems use a uniform light source that transilluminates the film and a 2D imaging system (2D CCD camera, for example) that measures light transmission over the entire plane simultaneously. The measured optical density represents a convolution of the densitometer light source emission spectrum, the film absorption spectrum, as well as the spectral sensitivity of the densitometer's detector. As a result, different densitometers produce different sensitometric curves for the same film type, radiation quality, and the dose range under investigation.

Dose measurements based on any film dosimetry system have uncertainties pertinent to a particular system used. By using a uniform radiation field during the calibration procedure, one attempts to create a situation where the measurement uncertainty is limited by only three factors: (1) the overall uncertainty of the reference dose measurement in the phantom; (2) the uncertainty due to nonuniform thickness of the sensitive layer; and (3) type A and B uncertainties associated with the densitometer used to measure the optical density (for a classification of uncertainties, see Ref. 20).

The goal of our study was to compare the sensitivity curves obtained for the HS and XR-T types of GafChromic films in conjunction with seven different densitometers. In addition, considering the densitometer/film system as a two-dimensional dosimeter, a practical uncertainty analysis was carried out that allows the estimation of uncertainty in dose determination due to the performance of the dosimetry system (experimental uncertainty) and the uncertainty introduced by the fit that is needed to convert measured optical density into the absorbed dose (fit error).

II. MATERIALS AND METHODS

A. New radiochromic films

Both the HS and XR-T GafChromic film models (International Specialty Products, Wayne, NJ) consist of single active layer sandwiched between two sheets of clear, transparent polyester, each with a thickness of approximately $97\ \mu\text{m}$ and a density of $1.35\ \text{g}/\text{cm}^3$. Both²¹ films use the same mixture of diacetylene monomer crystals suspended in a gelatin emulsion and have an active layer thickness of about $40\ \mu\text{m}$ for

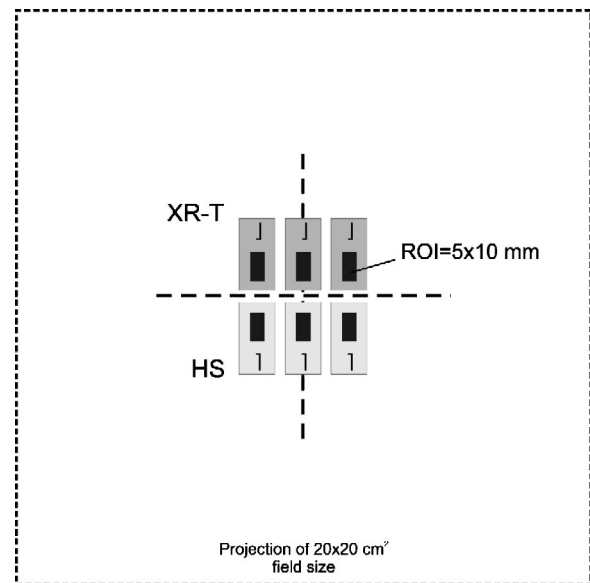


FIG. 1. Film irradiation geometry and definition of region of interest (ROI) over which the netODs have been analyzed: the ROI is a $5\ \text{mm} \times 10\ \text{mm}$ rectangle; the bottom half of the film was used for labeling and manual handling.

HS and about $30\ \mu\text{m}$ for XR-T model GafChromic film. The active layer mass densities are $1.08\ \text{g}/\text{cm}^3$ for the HS and $1.75\ \text{g}/\text{cm}^3$ for the XR-T films. The HS active layer nominally consists of: H-9%, C-57%, N-16%, O-18.0% by weight; while that of the XR-T nominally consists of: H-8%, C-46%, N-12%, O-14%, Cs-13%, and Br-8%.²¹ The purpose of the high atomic number Cs and Br additives is to increase a low energy photon response via the photoelectric-effect. The batch numbers used were I0144HS for HS film and 30198-1B for XR-T film.

B. Phantom and irradiation procedures

The sensitivity, defined as the netOD of the film per unit absorbed dose, was measured with doses ranging from 0 Gy to 50 Gy. Measurements were performed by irradiating film samples ($2.5\ \text{cm} \times 1.5\ \text{cm}$ in size) with the 6 MV photon beam from a Varian 2300 (C/D) accelerator (Varian, Palo Alto, CA). The films were exposed perpendicularly to the radiation beam in a $30\ \text{cm} \times 30\ \text{cm} \times 25\ \text{cm}$ solid water RMI-457 phantom using the geometry illustrated in Fig. 1. The figure also shows the regions of interest (ROI) that were used for the measurement of optical density change with dose. The ROI was a $5\ \text{mm}$ by $10\ \text{mm}$ rectangle in the upper half of the film piece, positioned $5\ \text{mm}$ from the film edges, to avoid OD measurement artifacts that have been observed near film edges.¹⁴ The bottom half of the film was used for labeling and manual handling. In our analysis we ignored the possible variations in mean sensitivity of different ROIs that were reported previously for the MD-55-2 model GafChromic film.¹²

Samples of film were placed at the isocenter plane of the LINAC, in a source-to-axis distance (SAD) setup at a distance of $100\ \text{cm}$. A $20\ \text{cm} \times 20\ \text{cm}$ field size at the isocenter

was used. The films were covered with a 5 cm thick piece of solid water and a 20 cm thick piece of solid water was placed below the films, to provide sufficient backscatter.

Three sets of films were prepared for distribution among different institutions involved in the study. Each set consisted of two film packets, one for each film type. Each film packet contained 16 pieces of film, which were exposed to the following doses: 0, 0.5, 1, 2, 3, 4, 5, 7.5, 10, 15, 20, 25, 30, 35, 40, and 50 Gy in our department. Reference doses were determined according to the TG-51 protocol,²² converted to dose-to-tissue. The output of the linac was measured before and after the irradiations, and a variation of 0.06% was observed. The film samples were handled in accordance with the recommendations outlined in the AAPM TG-55 report.²³ For each dose point, 6 pieces of films (3 for the HS model and 3 for the XR-T model) were positioned, as shown in Fig. 1.

One set of films was sent to the National Institute of Standards and Technology (NIST) and another to the Virginia Commonwealth University, where they were scanned 48 h after irradiation. The third set of films was read after 48 h in our center. Our film packets were then taped onto two separate transparencies and sent to eRadlink Inc. to be read 72 h postirradiation. The films were then sent to the Memorial Sloan-Kettering Cancer Center (MSKCC) and read 96 h postirradiation. The films were only removed from their light-protecting envelope during irradiation and readout to reduce the ambient light effects.²⁴

GafChromic films have shown to produce a relatively small variation in the optical density when the light source is fully linearly polarized and the film is rotated through a 360° angle.^{13,23,25} However, if both the light source and the detector are linearly polarized, variations in the measured optical density can reach 15% for the HS model GafChromic film²⁵ when the film is rotated through a 360° angle. In order to avoid the influence of this polarization effects on our comparison (when the laser light source densitometers are used, e.g., Molecular Dynamics, LKB Pharmacia, LaserPro16), we have cut and label the films always in the same way, so that the corner cut mark on a film sheet was in the upper right corner with respect to the long axis of the film pieces.

C. Densitometric systems

The objective of our study was to make a quantitative comparison between six commercially available densitometers as well as a LED diode spot densitometer used for GafChromic film dosimetry. As previously stated by McLaughlin and Desrosiers:²⁶ “A dosimetry system implies not only the radiation sensor itself but also the analytical methods that relate reproducibility of the radiation-induced signal to the absorbed dose at a location in a given material.” Accordingly, a GafChromic film dosimetry system should be understood as an ensemble of the film type, the scanning densitometer and the scanning protocol. The scanning protocol we used in our study was designed to provide a comparison of the raw densitometric data that each of the scanning systems can produce. To ensure that comparable data was

acquired for each scanner, the same protocol was used at all sites and some well-known techniques to improve precision in film dosimetry (for example, double exposure,^{12,13} multiple scans of the same film piece,²⁷ multiple sets of calibration packets) were neglected. Consequently, results presented in this work do not necessarily correspond to the best dosimetric results achievable by any one of the participating co-authors.

The following three point-detector type transmission densitometers were tested: (1) LKB Pharmacia UltraScan XL (at the National Institute of Standards and Technology, NIST) (In this paper, certain commercially available products are referred to by name. These references are for informational purposes only and do not imply that these products are the best or only products available for the purpose, and do not imply endorsement by NIST.); (2) Molecular Dynamics Personal Densitometer (at Virginia Commonwealth University, VCU); and (3) Nuclear Associates Radiochromic Densitometer Model 37-443 (at McGill University). Densitometer systems using 1D or 2D optical detectors investigated in this study were: (1) Photoelectron Corporation CMR-604 (NIST); (2) Laser Pro 16 (at eRadlink Inc., California); (3) Vidar VXR-16 (at MSKCC); and (4) AGFA Arcus II document scanner (at McGill University).

1. Nuclear Associates Radiochromic Densitometer, Victoreen Model 37-443

This system employs a filtered LED-diode spot densitometer (distributed by Nuclear Associates Inc., Carle Place, NY, from here on referred to as Victoreen) with an optimally designed (to the absorption spectrum of the GafChromic film) light source, which gives a high intensity spectrum centered at 671 nm. The 2 mm diameter aperture is coupled to an 11 nm band pass filter centered near the major peak of the GafChromic film absorption spectrum (675 nm). The system has a dynamic range of measurable optical densities from 0 to 4.00, with a stated accuracy of ± 0.02 over the specified range. The sensor is a high efficiency silicon photodiode. The system comes with a manual two-dimensional film transport system. Its micrometerlike design provides a precise method of holding and moving the film over the aperture of the densitometer in both x and y directions. The micrometer movement and the device's scale provide an x - y axis precision of ± 0.1 mm.

Because the aperture of this densitometer is 2 mm, we have performed the measurements by taking five readings within the ROI. The mean values and standard deviations have been calculated and used for the intercomparison with the other systems.

2. Agfa document scanner, Model Arcus II

Although not designed for GafChromic film dosimetry, document scanners have been used earlier for measurements in various film dosimetry applications.^{28,29} The Agfa Arcus II, no longer commercially available, is a desktop flat-bed document scanner designed for high quality photographic image scanning with an option to operate in a transmission mode. The scanner has a maximum resolution of 600 by

1200 dpi. It employs a fluorescent light source with a broad-band emission spectrum. The maximum scanning area when working in the transparent mode is 203 mm×254 mm. As a detector this scanner uses a linear 10 600-element color type CCD array.

Every film packet (for a given energy and film type) was scanned, together with an opaque piece of film as well as a step wedge film. This is the regular procedure in our center to keep track of the system's response linearity. Films are scanned using the Agfa FotoLook 3.5 software, with the OD range set to maximum and with all filters and image enhancement options turned off. Films have been scanned in the 48-bit RGB mode (16 bits per color) and saved as tagged image file format (TIFF) image files. Images were imported into in-house-written image manipulation routines, using MatLab 6.5.0 (Math Works, Natick, MA) that extracted only the red component of the RGB scanned image.

A scanning resolution of 300 dpi (85 μm per pixel) was used, which means that the 5 mm×10 mm ROI consists of 60×120 points. The mean value as well as the standard deviation over the ROI were taken and used for intercomparison.

3. Vidar VXR-16 DosimetryPRO™ Film Digitizer

The VXR-16 DosimetryPRO™ Film Digitizer (Vidar Systems Corporation, Herndon, Virginia, from here on referred to as Vidar VXR-16) has a fluorescent white light source with a spectral emission range between 250 nm and 750 nm. It is coupled to a linear CCD digitizing system. The digitizer can accommodate films of up to 35.56 cm wide and 43.18 cm long in size and produces images 16 bits deep (65536 shades of gray). The resolution of the device can be set to 89, 187, and 356 μm per pixel.

Each film in a packet was taped onto transparency paper (subtracted as background) and scanned using the RITT 3.1.11 software. The resolution used was 356 μm per pixel. The mean and standard deviations have been determined over the ROI (14×28 points) and used for the intercomparison.

4. LKB Pharmacia UltraScan XL

This instrument (from here on referred to as the LKB Pharmacia), no longer commercially available, is of the point-by-point translation type and employs a 0.1 mm diameter He-Ne laser for densitometry measurements. The step size in both x and a y direction is controllable in increments of 0.04 mm to a maximum of 0.6 mm. For our measurements a step size of 0.48 mm was used over the 5 mm×10 mm area of interest. The signal resolution is 12 bits (4096 shades of gray) over an optical density range of 4. Each film was read individually, mounted in the same area of the ground glass base plate of the system. The data used for the intercomparison are the average net pixel values over the ROI (10×20 points).

5. Photoelectron Corporation CMR-604

This instrument (from here on referred to as PeC), no longer commercially available, is of imaging type and employs a 242×375 element cooled CCD array to image light transmitted through the film. The film is backlit by a 665 nm LED array mounted beneath a white diffusing plate. Pixel sizes are governed by the position of the CCD camera above the film and the focusing lens. With the proper lens, a maximum resolution of 0.01 mm per pixel is achievable. For the measurements presented here, a pixel size of 0.075 mm was used. The signal resolution is 16 bits (65536 shades of gray), so the device has superior performance at low absorbance values. Each film was read individually, mounted in the same area of the system light box. The data used for the comparison are the average net pixel values over the ROI (66×132 points).

6. RadLink Laser Pro 16 Film Digitizer

The RadLink Laser Pro 16 Film Digitizer (eRadlink Inc. Systems Corporation, from here on referred to as LaserPro 16) employs a solid-state laser with the emission line centered at 658 nm. It is coupled to a linear solid-state silicon type detector, having up to 3072 pixels per scan line. The digitizer can accommodate films of up to 35.5 cm×43.2 cm in size, and produces images 16 bits deep. The spatial resolution of the device is variable from a minimum of 116 μm per pixel.

Every film packet in our study, taped onto transparency paper, was scanned using the eRadlink Image Acquire™ acquisition and analysis software. The resolution used in this study was 173 μm per pixel. The mean and standard deviations have been determined over the ROI (29×58 points) and used for the intercomparison.

7. Molecular Dynamics, PD Densitometer

A detailed description of the transmission scanning-laser film digitizer (Molecular Dynamics, Sunnyvale, CA, Personal Densitometer, from here on referred to as Molecular Dynamics) can be found in a comprehensive study by Dempsey *et al.*¹⁴ which deals with removing image artifacts caused by the coherent light source geometry imaging interference (Moiré) patterns. The device measures the charge produced in a photo-multiplier tube (PMT) by collecting 633 nm He-Ne laser light transmitted through the scanning bed and film to a collimated light-integrating cylinder. Spatial resolution along the translation axis is achieved by precision stepping of the scanning bed and laser beam. The device has two resolution settings of 50 μm or 100 μm pixels.

Data from the digitizer are stored as 12-bit words (integer values between 0 and 4095), corresponding to optical densities (OD) between 0 and 4.095, in a 16-bit TIFF format. The resolution used was 100 μm per pixel. The OD mean and standard deviations have been determined over the ROI (50×100 points) and used for the intercomparison.

Table I summarizes the basic characteristic of the densitometers used in our study. A more comprehensive set of

TABLE I. Specifications of densitometer systems used in this study.

Scanner	Light source		Detector type	Resolution	
	Type	Spectrum		Min. Spatial	Signal
Victoreen	LED diode	671 nm (11 nm FWHM)	Si Diode	2 mm	0.01
LaserPro16	Laser Diode	658 nm	Si type detector	116 μm	16-bit
Photoelectron Corp.	LED Diode	665 nm (20 nm FWHM)	CCD camera	10 μm	16-bit
AGFA Arcus II	Fluorescent Lamp ^a	broadband	linear CCD	21 μm	16-bit
Molecular Dynamics	He-Ne Laser	633 nm	PMT	50 μm	8/12-bit
VIDAR VXR-16	Fluorescent Lamp	broadband	linear CCD	89 μm	16-bit
LKB Pharmacia	He-Ne Laser	633 nm	PMT	100 μm	12-bit

^aIn this work, we used only the red component of the transmission RGB image.

densitometer properties for some of the densitometers used in this study can be found in the AAPM TG-55 report.²³

In this paper, we quote the vendor specified resolutions for densitometers and they may differ from those obtained experimentally.¹⁴

D. Dose uncertainty analysis

Film dose-response is usually expressed as the measured OD against the dose delivered to the film. However, to use the film for measurement of an unknown dose, dose is more conveniently plotted as a function of the measured netOD and the data can be fitted with an appropriate function using a least-squares method. This process is subject to uncertainties from two basic sources: one is of an experimental nature and the second is caused by the fit process and its parameters determined during the film calibration. The experimental uncertainties are caused by contributions from the netOD measurement reproducibility, registration of source with film, uncertainties in accelerator calibration, mismatch in temporal and thermal history of the film, differences in mean response from one piece of film to another, etc.

Below, we present a dose uncertainty analysis useful in conjunction with film as a technique to measure the absorbed dose. In this analysis we will only take into account the reproducibility in measuring the netOD as a contributor to the experimental uncertainty. The extension of the analysis including the other contributors listed above is then straightforward.

For the densitometers that do not read OD directly (AGFA Arcus II, LaserPro16, VIDAR 16) we define the netOD and the σ_{netOD} in the following way:

$$\text{netOD} = \text{OD}_{\text{exp}} - \text{OD}_{\text{unexp}} = \log_{10} \frac{I_{\text{unexp}} - I_{\text{bckg}}}{I_{\text{exp}} - I_{\text{bckg}}} \quad (1)$$

and, using the error propagation expression³⁰

$$\sigma_{\text{netOD}} = \frac{1}{\ln 10} \sqrt{\frac{\sigma_{I_{\text{unexp}}}^2 + \sigma_{I_{\text{bckg}}}^2}{(I_{\text{unexp}} - I_{\text{bckg}})^2} + \frac{\sigma_{I_{\text{exp}}}^2 + \sigma_{I_{\text{bckg}}}^2}{(I_{\text{exp}} - I_{\text{bckg}})^2}} \quad (2)$$

All quantities in Eqs. (1) and (2) are calculated over the same ROI, defined in Fig. 1: I_{unexp} is the intensity value of an unexposed film, I_{bckg} is the zero-light transmitted intensity

value measured with the opaque piece of film, I_{exp} is the read-out of the exposed film, and $\sigma_{I_{\text{unexp}}}$, $\sigma_{I_{\text{bckg}}}$, and $\sigma_{I_{\text{exp}}}$ are their corresponding standard deviations.

For the densitometers that read the OD directly, the netOD over the ROI for each sample was obtained by subtracting the zero dose optical density (OD_{unexp}) from the measured exposed film optical density, while the standard deviations in the netOD are obtained by summing in quadrature the standard deviations of exposed and unexposed pieces of film.

The zero dose readout, either I_{unexp} or OD_{unexp} , have been determined over the ROI as a weighted mean:

$$I_{\text{unexp}} = \frac{\sum_{i=1}^5 (I_{\text{unexp}_i} / \sigma_i^2)}{\sum_{i=1}^5 (1 / \sigma_i^2)}, \quad (3)$$

while the corresponding uncertainty was calculated as:

$$\sigma_{I_0}^2 = \frac{1}{\sum_{i=1}^5 (1 / \sigma_i^2)}, \quad (4)$$

where the summation is over the 5 unexposed film samples that were placed unexposed into each film packet.

Only in the case of the Molecular Dynamics scanner have film read-outs been carried out before the film exposures. In this case, the netOD was determined by the subtraction of the initial from the final value for every individual piece of film. While this should be a more accurate approach for other densitometers as well, we assume that this procedure does not introduce a significant difference in the data comparison.

For all 14-film model/scanner systems (7 scanners and two film types) we have plotted the delivered dose as a function of the measured netOD. In order to find the most suitable function for a given system, we used the following criteria: (i) the fit function has to be monotonically increasing; (ii) the fit function has to go through zero, and finally (iii) we choose the function that gives the minimum relative uncertainty for the fitting parameters. Based on these criteria, we have chosen the family of fit functions of the form

$$D_{\text{fit}} = a + b \cdot \text{netOD} + c \cdot \text{netOD}^n. \quad (5)$$

The third term in Eq. (5) was introduced to account for the nonlinear dose response while approaching the high dose region close to the saturation level for a given film dosimetry

system. The power n in Eq. (5) was treated as parameter and it was varied from 0.5 to 5.0 with a step of 0.5. For a given film type/densitometer combination, the n value leading to a minimal overall uncertainty was retained. We have also tried to leave the power n as a fitting parameter and observed that the sum of residuals would improve negligibly, if at all, by (for the best case) 0.2%. However, the introduction of a new fitting parameter has introduced higher fit uncertainties (by 1%–2%) in our analysis.

The fits of delivered dose (D) vs measured netOD change on the analytical forms given by Eq. (5) have been performed using the “Levenberg–Marquardt” quasi-Newton minimization method (TableCurve 2D 5.01.01, Systat, Point Richmond, CA), weighted using the following distribution:

$$w_i = \frac{1}{(\sigma_{\text{netOD}_i})^2} \cdot \frac{1}{\sum_i \frac{1}{(\sigma_{\text{netOD}_i})^2}} \tag{6}$$

The weighting distribution, as per Eq. (6), represents the relative experimental uncertainty of the measured netOD, so that the magnitude of the measured quantity does not dictate the weighting process.

In order to predict the uncertainty in the measurement of an unknown dose while using the calibration curve for each dosimetry system, we have used the expression for error propagation:³⁰

$$\sigma_y^2 = \sum_i \left(\frac{\partial y}{\partial x_i} \right)^2 \cdot \sigma_{x_i}^2 \tag{7}$$

assuming the absence of cross-correlation terms. In the above equation, σ_y is the total estimated uncertainty (stan-

dard deviation) for a dose determined using Eq. (5), while σ_{x_i} ($i=1,2,3$) represent the standard deviations for the netOD and the two fitting parameters b and c ; a was always forced to be 0.

From Eqs. (5) and (7), it follows (bearing in mind that $a=0$):

$$\sigma_{D_{\text{fit}}}^2 = \text{netOD}^2 \cdot \sigma_b^2 + \text{netOD}^{2n} \cdot \sigma_c^2 + (b + n \cdot c \cdot \text{netOD}^{n-1})^2 \cdot \sigma_{\text{netOD}}^2 \tag{8}$$

If we separate the terms related to the experimental uncertainty of the measured netOD (σ_{netOD}), for the selected fit functional form, we get

$$\sigma_{D_{\text{exp}}}(\%) = \frac{\sqrt{(b + n \cdot c \cdot \text{netOD}^{n-1})^2 \cdot \sigma_{\text{netOD}}^2}}{D_{\text{fit}}} \cdot 100 \tag{9}$$

However, as can be seen from Eq. (9), $\sigma_{D_{\text{exp}}}$ is a function of the optical density measurement uncertainty (σ_{netOD}) and also depends on the functional form in Eq. (5).

Terms in Eq. (8) related to the fitting parameter uncertainties (σ_b, σ_c) can be grouped as:

$$\sigma_{D_{\text{fit}}}(\%) = \frac{\sqrt{\text{netOD}^2 \cdot \sigma_b^2 + \text{netOD}^{2n} \cdot \sigma_c^2}}{D_{\text{fit}}} \cdot 100 \tag{10}$$

Fit uncertainty ($\sigma_{D_{\text{fit}}}$), defined by Eq. (10), is a function of the fit parameter uncertainties for the selected functional form in Eq. (5).

Finally, the total uncertainty for the dose measured using the above described formalism, for a particular functional form given by Eq. (5), is calculated as

$$\sigma_{D_{\text{tot}}}(\%) = \frac{\sqrt{\text{netOD}^2 \cdot \sigma_b^2 + \text{netOD}^{2n} \cdot \sigma_c^2 + (b + n \cdot c \cdot \text{netOD}^{n-1})^2 \cdot \sigma_{\text{netOD}}^2}}{D_{\text{fit}}} \cdot 100 \tag{11}$$

As pointed out above, Eq. (11) was derived taking into account only the uncertainties in the measured netOD as well as the uncertainties imposed by the fitting procedure of the dose vs netOD calibration curve.

It should be noted that in Eq. (7) correlations between fit parameters and the uncertainty on measured optical density were ignored. We verified that this is justified for the sub-selection of the fit functions used. In fact, the functional form of the fit is only needed to transform the relative uncertainty on the netOD into a relative uncertainty on the dose using the uncertainty propagation, given by Eq. (7).

III. RESULTS AND DISCUSSION

A. Performance of GafChromic film dosimetry systems

Figure 2 displays the dose sensitivity curves (left) for both film types (HS and XR-T) as a function of dose for 6 MV

photons together with the corresponding error bars. Dose sensitivity is defined as the net optical density divided by the dose that caused this OD change. The error bars represent twice the sum in quadrature of a constant 3% relative uncertainty in dose measurements and of the relative netOD measurements uncertainty (σ_{netOD}). The latter uncertainties are also presented for the seven densitometers used in this comparison on the right graphs in the same figure. Lines in Fig. 2, showing sensitivity data, represent the values calculated by dividing the measured netOD with the predicted doses determined from the fit curves, of Eq. (5), for a given film type/densitometer combination. It can be seen from Fig. 2 that for the HS film type, an agreement between measured and predicted sensitivity starts at approximately 2 Gy, whereas for the XR-T film type, the agreement between experiment and model is within the experimental error bars for doses above 3 Gy. This can be explained by the fact that the

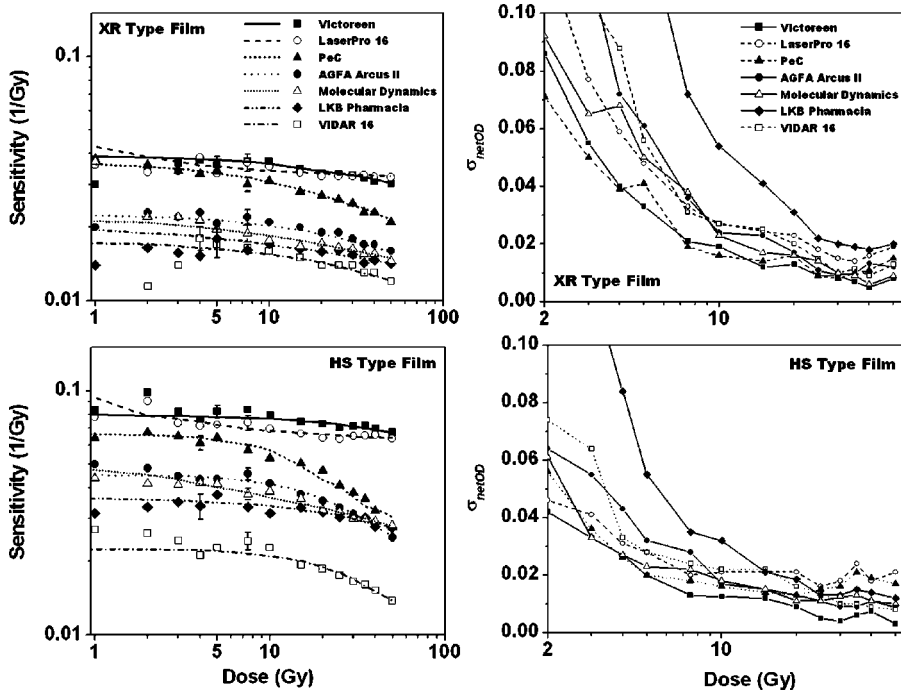


FIG. 2. Dose sensitivity curves for HS (lower-left) and XR-T (upper-left) film types as a function of delivered dose for 6 MV photon beam. Relative errors of the netOD measurements for HS (lower-right) and XR-T (upper-right) film types.

relative errors in the netOD measurements (Fig. 2, right) are higher for XR-T than for the HS type GafChromic film.

As a result of its highly customized light source for GafChromic film dosimetry, the filtered LED-diode spot densitometer shows the highest sensitivity. Doses to achieve a net optical density of 1 are 13 Gy for the HS film and 30.3 Gy for XR-T type GafChromic film. Comparing these results with previously published data for the MD-55-2 film model, which showed that a dose of 16 Gy was necessary to achieve a net optical density of 1 with the same densitometer,²⁷ it can be concluded that the HS type film has a somewhat higher sensitivity, while the XR-T film has a lower sensitivity than the MD-55-2 film when measured with the Victoreen densitometer. This means that the HS type film has by 20% higher sensitivity, while the XR-T film has a lower sensitivity (by 50%) than the MD-55-2 film when measured with the Victoreen densitometer.

In order to make a quantitative comparison among the GafChromic film dosimetry systems used in this study, we

have determined the dose required to achieve a net optical density of 0.5 when the pieces of film have been irradiated with the 6 MV photon beam. The results are summarized in Table II. Among the automated 2D scanning systems, the most sensitive dose response for GafChromic films was found with the LaserPro16 with its red solid-state laser line centered at 658 nm. This is followed by the PeC with its red LED diode sources centered at 665 nm. Three digitizing systems, Molecular Dynamics, LKB Pharmacia, and Agfa Arcus II are grouped in the same sensitivity range. When using the Agfa scanner we used the red component (extracted *a posteriori* from the 48-bit RGB raw image during the image analysis) of the wideband fluorescent lamp, while the two others employ the He-Ne laser, centered in a region between the two main absorption peaks of the GafChromic film absorption spectrum. The previously reported low sensitivity^{27,31} of the Vidar VXR-16, among the scanners used in

TABLE II. Dose in Gy to achieve a net optical density of 0.5 and relative error in net optical density measurements (averaged for doses above 5 Gy) for two film types exposed to a 6 MV photon beam.

Scanner	HS film		XR-T film	
	D(netOD=0.5) (Gy)	σ_{netOD} (%)	D(netOD=0.5) (Gy)	σ_{netOD} (%)
Victoreen	6	1.0	14	1.4
LaserPro16	7	2.2	15	2.3
PeC	10	1.7	21	1.6
AGFA Arcus II	12	1.5	28	2.2
Molecular Dynamics	14	1.4	31	1.9
LKB Pharmacia	15	2.4	35	4.3
VIDAR 16	30	1.6	44	2.2

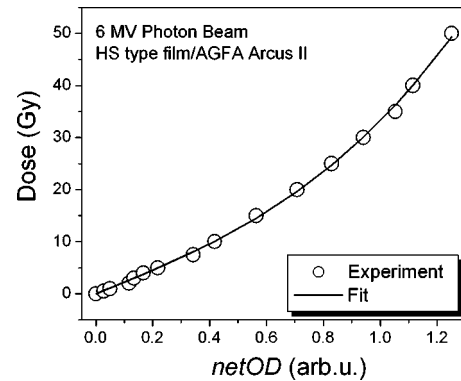


FIG. 3. Dose vs netOD for HS film and the AGFA Arcus II dosimetric system exposed to a 6 MV photon beam. Points are experimentally measured values while the line corresponds to the result of the fitting procedure.

TABLE III. Best fitting functions for different film type/densitometer combinations ($y \equiv \text{Dose}$ and $x \equiv \text{netOD}$).

Scanner	Fitting functions	
	HS film	XR-T film
LKB Pharmacia	$y = bx + cx^2$	$y = bx + cx^{1.5}$
VIDAR 16	$y = bx + cx^3$	$y = bx + cx^2$
Victoreen	$y = bx + cx^2$	$y = bx + cx^2$
PeC	$y = bx + cx^3$	$y = bx + cx^2$
Molecular Dynamics	$y = bx + cx^{1.5}$	$y = bx + cx^{1.5}$
LaserPro16	$y = bx + cx^{0.5}$	$y = bx + cx^{0.5}$
AGFA Arcus II	$y = bx + cx^3$	$y = bx + cx^2$

our study, is confirmed and it can be explained by the use of a broadband fluorescent light source by the Vidar densitometer. The same table also summarizes the relative errors for the netOD measurements using seven different densitometers. The relative netOD error values listed in the table represent averaged relative errors in netOD values for doses higher than 5 Gy.

B. Comparison of dose-uncertainty performances

Figure 3 represents one example of the calibration procedure for the 6 MV photon beam, using the HS film/AGFA Arcus II scanner combination. The experimental points are presented together with the result of the fitting procedure.

The list of the best fitting functions for different film type/densitometer combinations is given in Table III. The functional forms have been determined based on the criteria explained in Sec. II D. The power n in Eq. (5) was varied from 0.5 to 5 with the step of 0.5. We have verified that the residuals for all the fit functions listed in Table III, follow the Gaussian distribution. Accordingly, it was justified that the experimental data are randomly scattered about the line of the best fit, in which case standard deviation parameter, calculated using Eq. (11) is a proper measure of the uncertainty in dose determination.

We now assume that the data we have obtained to perform the calibration curve fittings represent netOD measurements for unknown doses. Using the expression given by Eq. (11), we calculated the total uncertainty estimate in the “unknown” dose determination using the calibration curve given

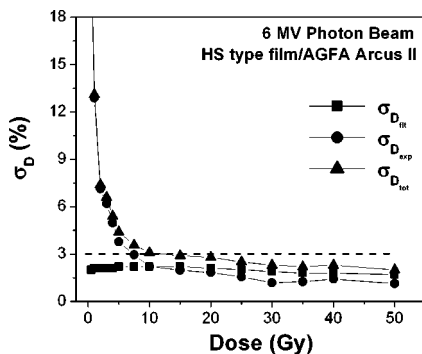


FIG. 4. Dose measurement uncertainties for the HS film/AGFA Arcus II system exposed to 6 MV photon beam.

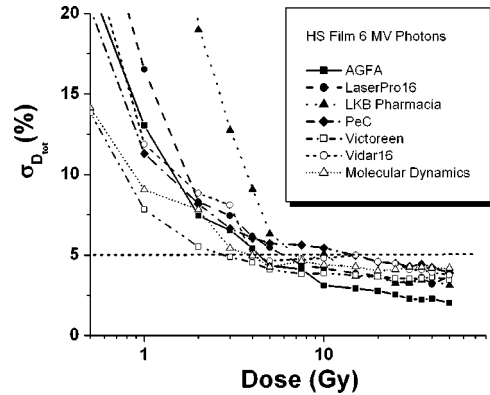


FIG. 5. Total uncertainties for the measured dose by using different densitometers in combination with HS type GafChromic film for 6 MV photons.

by Eq. (5). Figure 4 summarizes components of the uncertainty for the dose determined by using the HS film/AGFA Arcus II system for the 6 MV photon beam. This graph represents typical behavior for all other film type/scanner combinations. It shows that the fit uncertainty, calculated using Eq. (10), is approximately constant while the experimental uncertainty, calculated using Eq. (9), drops exponentially with an increasing dose. For the example shown in Fig. 4, one may conclude that for a given GafChromic film dosimetry system, a 3% overall uncertainty level can be achieved, based on a single exposure measurement, for doses above 10 Gy.

Figure 5 shows the total uncertainty, calculated using Eq. (11), in the measured dose range using different densitometers in combination with the HS type GafChromic film for 6 MV photons. Although the sensitivity curves are most often used to compare dosimetric abilities of different film dosimetric systems, we believe that Fig. 5 more directly and quantitatively describes the potential dosimetric precision of the RCF-densitometry combination. All systems reach the 5% uncertainty level in a dose range between the 3 and 15 Gy.

In order to make a quantitative comparison among the scanners used in this study, we have tabulated results of the error analysis in Tables IV and V.

Table IV shows dose values in Gy at which total uncertainty, given by Eq. (11), in dose determination falls below 5%. The minimum doses to reach the 5% uncertainty level are determined by the intersection of the fitted total uncertainty vs dose curves (using different exponentially decaying

TABLE IV. Dose, in Gy, at which the total dose uncertainty falls below 5%.

Scanner	HS film	XR-T film
Victoreen	3	5
Molecular Dynamics	5	7
AGFA Arcus II	5	7
PeC	5	8
VIDAR 16	6	7
LaserPro16	6	8
LKB Pharmacia	7	never

TABLE V. The average uncertainty by source (experimental or fit) for doses higher than 5 Gy.

Scanner	HS film		XR-T film	
	Expt.	Fit	Expt.	Fit
Victoreen	1%	4%	1%	3%
AGFA Arcus II	2%	2%	2%	2%
Molecular Dynamics	2%	3%	2%	3%
LaserPro16	2%	3%	2%	3%
PeC	2%	4%	2%	3%
VIDAR 16	3%	4%	3%	2%
LKB Pharmacia	3%	3%	5%	7%

functions) with the 5% total uncertainty level. The scanners in Table IV have been sorted with respect to increasing minimum dose to reach 5% uncertainty level for the HS film type.

Since the results in Table IV include the error contributions due to both the experiment and the fitting procedure, we have decided to extract the experimental uncertainties in a separate table. The reason for this is that the experimental uncertainties are pertinent to the film type/scanner system and are characteristic of a single measurement. A single measurement is what can be expected to be the case in most experimental measurement applications, once the system has been calibrated.

Table V shows the mean uncertainty in dose determination by the source of uncertainty (experimental or fit) for the HS and XR-T film types, respectively, for doses higher than 5 Gy. Averages have been taken for both experimental and fit uncertainties over the dose points in the dose range from 5 Gy to 50 Gy. The dose of 5 Gy was taken arbitrarily for the sake of qualitative comparison among the scanners under investigation. The scanners have been sorted based on the experimental uncertainty for the HS type film.

The results of our analysis, summarized in Tables IV and V, do not represent the best possible dosimetric performances of a particular film type/scanner system. An appropriate protocol should be developed for each of the film type/scanner combinations at a given beam modality in order to build the best achievable GafChromic film dosimetry system.

IV. CONCLUSIONS

Based on our comparisons among the seven commercially available digitizers for the GafChromic film dosimetry in the dose range from 0 Gy to 50 Gy, the Victoreen spot densitometer, specifically designed for the RCF dosimetry, has the highest sensitivity. A dose to achieve a net optical density of 0.5 for the HS film type irradiated in a 6 MV photon beam ranges from 6 Gy for the Victoreen to 30 Gy for the Vidar VXR-16 densitometer. Variation in the sensitivity response among the GafChromic film dosimetry systems is mainly governed by the difference in the emission spectra between different densitometers. A set of best dose vs netOD fitting functions for the different film type/densitometer combinations was obtained and it was found that these functions depend on the given system film type/scanner.

This study has considered two sources of type A uncertainties, characteristic of the GafChromic film dosimetry process: experimental uncertainty caused by the act of measurement and uncertainty in the function fitting parameters, which are determined during the calibration process. Among the scanners used in this comparison and for the HS film type, the experimental uncertainty varies from 1% to 3%, while the calibration fitting uncertainty ranges from 2% to 4% for doses above 5 Gy. Despite the observed significant variation of sensitivity, the studied densitometers exhibit a very similar precision for GafChromic film measurements above 5 Gy with the protocol used in this study.

Finally, the comparative results presented in this paper would serve as guidelines for the GafChromic film dosimetry system characteristics. Every system has its own limitations that have to be understood and established during the calibration procedure. Methods pertinent to a particular system (multiple calibration film batches, multiple scans, etc.) should be developed as a part of the GafChromic film dosimetry protocol for a given system.

ACKNOWLEDGMENTS

We would like to thank Dr. David Lewis from ISP for useful discussions. J.S. is a research scientist of the National Cancer Institute Canada appointed with funds provided by the Canadian Cancer Society.

^{a)}Author to whom correspondence should be addressed. Phone: 514-934-8052; fax: 514-934-8229; electronic mail: devic@medphys.mcgill.ca

¹W. L. McLaughlin, J. C. Humphreys, D. Hocken, and W. J. Chappas, "Radiochromic dosimetry for validation and commissioning of industrial radiation processes," in *Progress in Radiation Processing*, Proceedings of the Sixth International Meeting, Ottawa, 1987, edited by F. M. Fraser [Radiat. Phys. Chem. **31**, 505–514 (1988)].

²M. C. Saylor, T. T. Tamargo, W. L. McLaughlin, H. M. Khan, D. F. Lewis, and R. D. Schenfele, "A thin film recording medium for use in food irradiation" [Radiat. Phys. Chem. **31**, 529–536 (1988)].

³R. D. H. Chu, G. Van Dyke, D. F. Lewis, K. P. J. O'Hara, B. W. Buckland, and F. Dinelle, "GafChromic dosimetry media: A new high dose rate thin film routine dosimeter and dose mapping tool," Radiat. Phys. Chem. **35**, 767–773 (1990).

⁴W. L. McLaughlin, Y. D. Chen, C. G. Soares, A. Miller, G. Van Dyke, and D. F. Lewis, "Sensitometry of the response of a new radiochromic film dosimeter to gamma radiation and electron beams," Nucl. Instrum. Methods Phys. Res. A **302**, 165–176 (1991).

⁵P. J. Muench, A. S. Meigooni, R. Nath, and W. L. McLaughlin, "Photon energy dependence of the sensitivity of radiochromic film compared to silver halide film and lithium fluoride TLDs," Med. Phys. **18**, 769–775 (1991).

⁶G. Soares, "Calibration of ophthalmic applicators at NIST: A revised approach," Med. Phys. **18**, 787–793 (1991).

⁷M. Farahani, F. C. Eichmiller, and W. L. McLaughlin, "A new method for shielding electron beams used for head and neck cancer treatment," Med. Phys. **20**, 1237–1241 (1993).

⁸W. L. McLaughlin, C. G. Soares, J. A. Sayeg, E. C. McCullough, R. W. Kline, A. Wu, and A. H. Maitz, "The use of a radiochromic detector for the determination of stereotactic radiosurgery dose characteristics," Med. Phys. **21**, 379–388 (1994).

⁹M. J. Butson, J. N. Mathur, and P. E. Metcalfe, "Radiochromic film as a radiotherapy surface-dose detector," Phys. Med. Biol. **41**, 1073–1078 (1996).

¹⁰W. L. McLaughlin, J. M. Puhl, Al-Sheikhly, C. A. Christou, A. Miller, A. Kova'cs, L. Wojna'rovits, and D. F. Lewis, "Novel radiochromic films for clinical dosimetry," in *Proceedings of the 11th International Confer-*

- ence on Solid State Dosimetry, II*, Budapest, July, 1995, edited by A. Peto and G. Uchrin [Radiat. Prot. Dosim. **66**, 263–268 (1996)].
- ¹¹ A. S. Meigooni, M. F. Sanders, G. S. Ibbott, and S. R. Szeglin, “Dosimetric characteristics of an improved radiochromic film,” *Med. Phys.* **23**, 1883–1888 (1996).
 - ¹² Y. Zhu, A. Kirov, A. Mishra, A. Meigooni, and J. Williamson, “Quantitative evaluation of radiochromic film response for two-dimensional dosimetry,” *Med. Phys.* **24**, 223–231 (1997).
 - ¹³ N. Klassen, L. Zwan, and J. Cygler, “GafChromic MD-55: Investigated as a precision dosimeter,” *Med. Phys.* **24**, 1924–1934 (1997).
 - ¹⁴ J. F. Dempsey, D. A. Low, A. S. Kirov, and J. F. Williamson, “Quantitative optical densitometry with scanning-laser film digitizers,” *Med. Phys.* **26**, 1721–1731 (1999).
 - ¹⁵ S. Pai, L. E. Reinstein, G. Gluckman, Z. Xu, and T. Weiss, “The use of improved radiochromic film for in vivo quality assurance of high dose rate brachytherapy,” *Med. Phys.* **25**, 1217–1221 (1998).
 - ¹⁶ M. J. Butson, P. K. N. Yu, and P. E. Metcalfe, “Extrapolated surface dose measurements with radiochromic film,” *Med. Phys.* **26**, 485–488 (1999).
 - ¹⁷ K. Y. Quach, J. Morales, M. J. Butson, A. B. Rosenfeld, and P. E. Metcalfe, “Measurement of radiotherapy x-ray skin dose on a chest wall phantom,” *Med. Phys.* **27**, 1676–1680 (2000).
 - ¹⁸ J. F. Dempsey, D. A. Low, S. Mutic, J. Markman, A. S. Kirov, G. H. Nussbaum, and J. F. Williamson, “Validation of a precision radiochromic film dosimetry system for quantitative two-dimensional imaging of acute exposure dose distributions,” *Med. Phys.* **27**, 2462–2475 (2000).
 - ¹⁹ M. J. Butson, T. Cheung, P. K. N. Yu, and P. E. Metcalfe, “Assessment of large single-fraction, low-energy x-ray dose with radiochromic film,” *Int. J. Radiat. Oncol., Biol., Phys.* **46**, 1071–1075 (2000).
 - ²⁰ Absorbed Dose Determination in External Beam Radiotherapy, Technical Report Series No. 398, International Atomic Energy Agency, Vienna, 2000.
 - ²¹ D. F. Lewis (private communication).
 - ²² P. R. Almond, P. J. Biggs, B. M. Coursey, W. F. Hanson, M. S. Huq, R. Nath, and D. W. O. Rogers, “AAPM’s TG-51 protocol for clinical reference dosimetry of high-energy photon and electron beams,” *Med. Phys.* **26**, 1847–1870 (1999).
 - ²³ A. Niroomand-Rad, C. R. Blackwell, B. M. Coursey, K. P. Gall, J. M. Galvin, W. L. McLaughlin, A. S. Meigooni, R. Nath, J. E. Rodgers, and C. G. Soares, “Radiochromic film dosimetry. Recommendations of AAPM Radiation Therapy Committee Task Group 55,” *Med. Phys.* **25**, 2093–2115 (1998).
 - ²⁴ M. J. Butson, P. K. N. Yu, and P. E. Metcalfe, “Effects of read-out light sources and ambient light on radiochromic film,” *Phys. Med. Biol.* **43**, 2407–2412 (1998).
 - ²⁵ M. J. Butson, P. K. N. Yu, T. Cheung, and D. Inwood, “Polarization effects on a high-sensitivity radiochromic film,” *Phys. Med. Biol.* **48**, N207–N211 (2003).
 - ²⁶ W. L. McLaughlin and M. F. Desrosiers, “Dosimetry systems for radiation processing,” *Radiat. Phys. Chem.* **46**, 1163–1174 (1995).
 - ²⁷ G. R. Gluckman and L. E. Reinstein, “Comparison of three high-resolution digitizers for radiochromic film dosimetry,” *Med. Phys.* **29**, 1839–1846 (2002).
 - ²⁸ H. Alva, H. Mercado-Urbe, M. Rodriguez-Villafuerte, and M. E. Brandan, “The use of a reflective scanner to study radiochromic film response,” *Phys. Med. Biol.* **47**, 2925–2933 (2002).
 - ²⁹ T. D. Bohm, D. W. Pearson, and R. K. Das, “Measurements and Monte Carlo calculations to determine the absolute detector response of radiochromic film for brachytherapy dosimetry,” *Med. Phys.* **28**, 142–146 (2001).
 - ³⁰ P. R. Bevington and D. K. Robinson, *Data Reduction and Error Analysis for the Physical Sciences* (WCB/McGraw-Hill, Boston, 1992).
 - ³¹ T. Cheung, M. J. Butson, and P. K. N. Yu, “Evaluation of a fluorescent light densitometer for radiochromic film analysis,” *Radiat. Meas.* **35**, 13–16 (2002).